

## Pressure estimation for diamond anvil cell under very-low pressures, hydrostatic conditions - re-evaluation for quartz Raman peak shifts -

\*Kazuki Kubo<sup>1</sup>, Kazuaki Okamoto<sup>1</sup>

1. Faculty of Education, Saitama University

Pressure shift of the ruby R1 luminescent has been used as primary pressure gauge in diamond-anvil experiments. However, the pressure calibration under low-pressure conditions (<1 GPa) was poorly constrained although crustal hydrothermal experiments are important. For calibration of the R1 luminescent shifts at low-pressure conditions, we have done diamond anvils experiments at room temperature conditions. H<sub>2</sub>O and ethanol were used as pressure transmitting medium and all experimental pressures was below ice stability field keeping hydrostatic-pressure conditions. We could get well-constrained new calibration line. Our new pressure estimation based on the quartz Raman peaks gives lower pressures than that of previous experiments reported by Schmidt and Ziemann (2000). For example, it would give 0.6 GPa from our experimental study although the previous study estimated at 1 GPa. This discrepancy causes significant overestimates for residual pressures determined by quartz Raman analysis from the natural rocks.

Schmidt, C., and Ziemann, M.A., 2000, *American Mineralogist*, v. 85, p. 1725–1734.

# Deformation history of Sanbagawa eclogites and their relation to Higash-Akaishi garnet peridotites

\*Satoshi KOGUCHI<sup>1</sup>, Ayumi Nishi<sup>1</sup>, Kana Koike<sup>1</sup>, Hafiz Ur Rehman<sup>1</sup>

1. Kagoshima University

We present Electron Back Scattered Diffraction (EBSD) maps and crystal preferred orientations (CPO) of the eclogites in the subduction-related high-pressure/low-temperature type Sanbagawa metamorphic belt, central Shikoku, Japan. The Sanbagawa metamorphic belt, extends over >800 km along the southwest Japan, bounded to the north by the Ryoke belt (a Cretaceous high-temperature and low-pressure regional metamorphic belt) along the Median Tectonic Line and to the south by the Chichibu and Shimanto belts, forming the well-known paired metamorphic belts of Miyashiro (1961).

Eclogites investigated in this study were collected from the Iratsu body in the Besshi area.

Our EBSD data reveal mainly L-type fabric (strongest CPO along [001]-axes and {011}-poles, suggesting intra-crystalline flow along [001]{110} and  $\langle 110 \rangle$ {110} slip systems) in omphacite, random or weak fabric in garnet, and almost an identical CPO to that of omphacite was observed in hornblende. In addition, actinolite shows irregular CPO pattern. The L-type fabric in omphacite and weak or irregular fabric of garnet indicate constrictive deformation under the eclogite facies stage. Hornblende was formed around omphacite however retained the original fabric from that of omphacite. Our results are consistent with the garnet and omphacite presented by Muramoto et al. (2011) for the garnet-peridotite from the Higashi-akaishi ultramafic body. Our results suggest that the ultramafics and eclogites experienced similar deformation regime therefore considering eclogites and garnet peridotites as separate tectonic blocks needs reappraisal.

## References

### Reference

Miyashiro, A. (1961). Evolution of metamorphic belts. *Journal of Petrology*, **2**, 277–311.

Muramoto et al. (2011). Rheological contrast between garnet and clinopyroxene in the mantle wedge: An example from Higashi-akaishi peridotite mass, SW Japan. *Physics of the Earth and Planetary Interiors* **184**, 14-33.

Keywords: Eclogite, Higashi Akaishi peridotite body, Sanbagawa metamorphic belt

# Mineralogical and petrological features of the Sanbagawa eclogites and amphibolites: pseudosection modelling

\*Ayumi Nishi<sup>1</sup>, Satoshi Koguchi<sup>1</sup>, REHMAN Ur Hafiz<sup>1</sup>

1. Kagoshima University

We present a summary on the mineralogical and petrological features of eclogites and amphibolites from the Sanbagawa metamorphic belt, southwest Japan. The Sanbagawa metamorphic belt, extending over > 800 km along the southwest Japan, bounded to the north by the Ryoke belt (a Cretaceous high-temperature and low-pressure regional metamorphic belt) along the Median Tectonic Line and to the south by the Chichibu and Shimanto belts, forming the well-known paired metamorphic belts of Miyashiro (1961). The belt is composed of basic, quartzose, pelitic-psammitic schists and several eclogites and ultramafic bodies. In this study, we investigated samples from the Iratsu eclogite body and Tonaru amphibolites for detailed mineralogical, petrological, and tried to understand the metamorphic history using the pseudosection modelling. Based on petrography, eclogite samples contain porphyroblastic garnets, highly cracked and surrounded by amphibole, quartz, chlorite, and epidote. Hornblende and clinopyroxene show penetrative along-strike foliation. Mineralogically garnets are weakly zoned and Alm-rich, and the contents of Grs increase slightly from core towards rim. Amphibole is mainly hornblende and actinolite with minor barroisitic composition. Pseudosection modelling, using THERMOCALC, was applied to constrain the metamorphic P-T path. The work is in progress, but preliminary results show a prograde path for eclogites which could have possible transformed into amphibolites during retrogression.

## Reference

Miyashiro, A. (1961). Evolution of metamorphic belts. *Journal of Petrology* 2, 277-311.

Keywords: Sanbagawa, Petrology, eclogite

## High-pressure epidote-amphibolites in the Yuli belt, eastern Taiwan: new thermobarometric constraints and petrological implications

\*Chiao Liu<sup>1</sup>, Chin-Ho Tsai<sup>1</sup>, Wen-Han Lo<sup>1</sup>

1. Department of Natural Resources and Environmental Studies, National Dong Hwa University, Hualien, Taiwan

Recent studies on Tamayen glaucophane schists show that metamorphic conditions of the Yuli belt might have been underestimated previously (Baziotis et al., 2017). Epidote amphibolites are closely associated with glaucophane schists, but P-T conditions of the former are less certain. We investigated a suite of Tamayen epidote amphibolites by computing equilibrium assemblage diagrams with the THERIAK/DOMINO software package. Peak mineral assemblage is garnet ( $\text{Alm}_{61-63}\text{Grs}_{17-18}\text{Prp}_{14-16}\text{Sps}_{03-05}$ ) + amphibole (pargasite) + epidote + paragonite + rutile + quartz. In rare cases, glaucophane rims on pargasite locally. The computed phase diagrams show that paragonite-in fields represent high-pressure conditions, although paragonite is not commonly considered as a high-pressure index mineral. Based on petrographic features, mineral compositions and computed equilibrium assemblage diagrams, peak P-T conditions are constrained as 13-15 kbar and 530-570 °C, which are compatible with those of Tamayen glaucophane schists. Both rock types represent metamorphic products in a subduction zone setting and were exhumed from depths of 40-50 km.

Keywords: equilibrium assemblage diagram, subduction zone, paragonite

## New geochronological constrains on high-pressure meta-plagiogranites in the Yuli belt, Taiwan: results from LA-ICP-MS zircon dating

\*Wen-Han Lo<sup>1</sup>, Chin-Ho Tsai<sup>1</sup>, Chiao Liu<sup>1</sup>

1. Department of Natural Resources and Environmental Studies, National Dong Hwa University, Hualien, Taiwan

We analyzed zircon separated from high-pressure meta-plagiogranites in the Chinshuichi mélange unit with LA-ICP-MS facilities. The mélange contains blocks of serpentinite, meta-gabbro, pillow-structured metabasite, epidote amphibolite and meta-plagiogranite in a matrix of meta-sediments. The meta-plagiogranites commonly contain meta-mafic enclaves, indicating an intrusive protolith origin. Glaucophane and omphacite occur in some of the meta-plagiogranites (Keyser et al., 2016). From the LA-ICP-MS analyses, three samples yielded mean  $^{206}\text{Pb}/^{238}\text{U}$  dates of  $13.1 \pm 1.9$  Ma,  $15.7 \pm 0.4$  Ma and  $16.3 \pm 1.4$  Ma. On the basis of zircon petrographic features (e.g. no obvious overgrowth in CL images), we conclude that the dates represent timing of magmatic crystallization of the meta-plagiogranites. These zircon ages place geochronological constraints on a late-stage shallow intrusion in a mid-Miocene oceanic section, which is likely of origin from the South China Sea domain.

Keywords: ophiolite, mélange, high-pressure metamorphism

## Fast and Slow Schists: Constraints from phengite geochronology

\*Tetsumaru Itaya<sup>1</sup>

1. Engineering Geology Center, Hiruzen Institute for Geology and Chronology

A systematic K-Ar age mapping along transects perpendicular to metamorphic thermal gradients have been carried out in the Sanbagawa *HP* schist belt in central Shikoku where the highest grade rocks occur in the middle part of the apparent stratigraphy. This reveals a positive correlation in age-*T* relationship that the ages are progressively older with increasing metamorphic temperature. It is impossible to explain the relationship based on the closure temperatures (CT) by the thermally activated diffusion model because CT would be much higher (ca. 600°C) than is currently generally accepted as revealed by the argon geochronology of the polymetamorphic terrains and because the metamorphic sequences formed in the temperatures lower than the CT. The *HP-UHP* schists have been deformed severely during the exhumation of their host rocks and the phengites have experienced the argon release from the phengite crystals by their dynamic recrystallization. The K-Ar ages are related directly to the ductile deformation history of the matrix phengite during exhumation and cooling of the schists. This suggests that the argon release cease when the ductile deformation of phengites stopped and the K-Ar ages are related to the timing of cease of ductile deformation. The coherent schist unit having an inverted thermal structure with large-scale recumbent folds may have undergone ductile deformation for a longer time at lower temperature, suggesting a relatively low strain rate for deformation of metamorphic pile. The duration of deformation during the exhumation after the peak metamorphism shows the average values from the peak metamorphism to the deformation ceasing level. It is 31 Myr in the biotite zone schists in the Sanbagawa *HP* schist belt in central Shikoku and much longer in the garnet and chlorite zone schists.

Multi-stage exhumation models have been proposed for *HP-UHP* metamorphic sequences. The models are that the exhumation rates were high from the deepest level to the lower crust and the rates decrease to the shallow crustal levels. In the Sanbagawa *HP* schist belt in central Shikoku, the eclogite facies metamorphic rocks exhumed faster than the lower grade rocks. The early stage of exhumation from the eclogite facies to the overprinting amphibolite facies gives 9 mm/y. The rates are much lower in the later stage of exhumation. Lago di Cignana *HP-UHP* units in the western Alps have very short duration of deformation, in particular, less than 5 Myr in Lago di Cignana *UHP* unit, suggesting the exhumation rate is higher than 18 mm/y in the early stage of exhumation from the deepest level (ca. 120 km) to the lower crust (ca. 30 km), being two times higher than that of the Sanbagawa *HP* schist belt. Lago di Cignana *HP-UHP* units and Sanbagawa *HP* schist belt both are Pacific-type *HP-UHP* metamorphic belts consisting of the metamorphosed oceanic lithology that usually record only a single metamorphic cycle though the former has been considered to be part of collisional orogeny. Lago di Cignana *HP-UHP* units having the higher exhumation rate are likely due to the subsequent continental collision event because Sanbagawa *HP* schist belt with the lower exhumation rate did not experience the subsequent continental collision event. Thus, the former with the high exhumation (strain) rate makes “Fast schist” sequence that the several unit boundaries are distinct fault and the later with the low exhumation (strain) rate, “Slow schist” sequence having the large scale recumbent fold.

Keywords: Pacific-type *HP-UHP* metamorphic belts, Exhumation rate, strain rate, phengite geochronology, Fast and Slow Schists

## Cathodoluminescence petrography of P-type jadeitites from the New Idria serpentinite body, California

\*Naoko Takahashi<sup>1</sup>, Tatsuki Tsujimori<sup>1</sup>, Masahiro KAYAMA<sup>2</sup>, Hirotsugu Nishido<sup>3</sup>

1. Tohoku University, 2. Department of Earth and Planetary Material Sciences, Faculty of Science, Tohoku University, 3. Department of Biosphere-Geosphere Science, Okayama University of Science

Because of strong emissions, cathodoluminescence (CL) observation is a powerful technique to characterize growth textures of nearly end-member jadeite. We applied this technique for a P-type (fluid precipitation) jadeite from the New Idria serpentinite body of the Diablo Range (California, U.S.A.). The investigated New Idria jadeite is a veined rock, consisting of pale-greenish jadeite matrix with numerous veins of white jadeite. Overall, nearly pure (> 95 mol%) jadeite crystal exhibits enough CL emissions for optical observations. The brightness of the emission divide into two contrasting portions, i.e., dark (pale-greenish matrix) and bright portions (veins). In the bright-CL portions, jadeite crystal shows a core-rim texture and/or an overgrowth texture; typically the blue-CL (or dull-blue-CL) cores are overgrown by the red-CL rims. Fine oscillatory growth, with rhythmic changes of red- and (dull-) blue-CL emissions, parallel to growth faces are also developed. Notably CL emissions from veins of older generation are somewhat obscure, likely due to intercrystalline deformation. The CL spectra shows broad overlapping peaks at ~320 and ~360 nm. In the blue-CL segments of jadeite crystals, intensity of these peaks is up to 10,000–120,000 arbitrary units (a.u.). In contrast, these of the red-CL segments of jadeite crystals reach up to 10,000–80,000 a.u. and have an additional peak at ~700 nm (5,000–70,000 a.u.). Electron microprobe analyses confirmed that less-bright CL-emission portions (dull-blue- or dark-CL) are more impure than the bright CL-emission portions (red- or blue-CL jadeites). Growth segments with blue or dull-blue-CL-emission has a higher aegirine component and TiO<sub>2</sub> than those with red-CL jadeites. The spectrum type (color) and brightness are basically controlled by impurities as CL activators.

Keywords: cathodoluminescence, jadeite

## Petrological comparison between Siberian and NW Pacific lithospheric mantle: A preliminary evaluation of the lithosphere stacking model

\*Shimbori Nozomi<sup>1</sup>, Tatsuki Tsujimori<sup>4</sup>, Naoto Hirano<sup>4</sup>, Jun-Ichi Kimura<sup>2</sup>, Vladimir Malkovets<sup>3</sup>

1. National University University Tohoku University, 2. Japan Agency for Marine-Earth Science and Technology, 3. VS Sobolev Institute of Geology and Mineralogy, Siberian Branch, Russian Academy of Sciences, 4. Center for Northeast Asian Studies

Understanding nature of subcontinental lithospheric mantle (SCLM) is of considerable importance as underscored by the abundance of studies in different Solid Earth Sciences, including petrology, geochemistry, volcanology, seismology, and geodynamics. So far many researchers have endeavored to accurately visualize heterogeneity of SCLM and its evolution. One possible model to form lithologic heterogeneity is the lithosphere stacking model proposed by Helmstaedt and Schulze (1989). In order to evaluate the model, two contrasting mantle peridotites from cratonic (continental) and oceanic lithospheres were investigated. Deformed garnet peridotite xenoliths from the Udachnaya kimberlite pipe, as a representative material of SCLM, record multiple mantle processes beneath a craton. In-situ trace elements analyses of garnet and clinopyroxene of the garnet peridotite, confirmed at least two times of mantle–melt interaction and possible fluid infiltration at the latest process. Comparing petrological features of Siberian SCLM xenolith together with an oceanic lithospheric mantle xenolith (spinel peridotite) from the Miyagi offshore petit spot volcano, the lithosphere stacking model was revisited. No matter whether the model is realistic or not, this study confirmed that deep SCLM materials contain geochemical and mineralogical evidences of the presence of “water”, likely supplied from deeply subducted oceanic lithosphere.

Keywords: lithospheric mantle, mantle xenolith, lithosphere stacking, trace element, garnet



## Magma sources and petrogenesis of middle Paleozoic ultramafic-mafic rocks from the east part of the Qilian block, NW China: Implications for subduction and underplating

\*Kuoan Tung<sup>1</sup>, Xian-hua Li<sup>2</sup>, Dunyi Liu<sup>3</sup>, Jianxin Zhang<sup>3</sup>, Chien-Yuan Tseng<sup>4</sup>

1. National Museum of Natural Science, Taiwan, 2. Institute of Geology and Geophysics, Chinese Academy of Sciences, 3. Institute of Geology, Chinese Academy of Geological Sciences (CAGS), Beijing 100037, People's Republic of China, 4. Department of Earth Sciences, National Cheng Kung University, Tainan 701, Taiwan

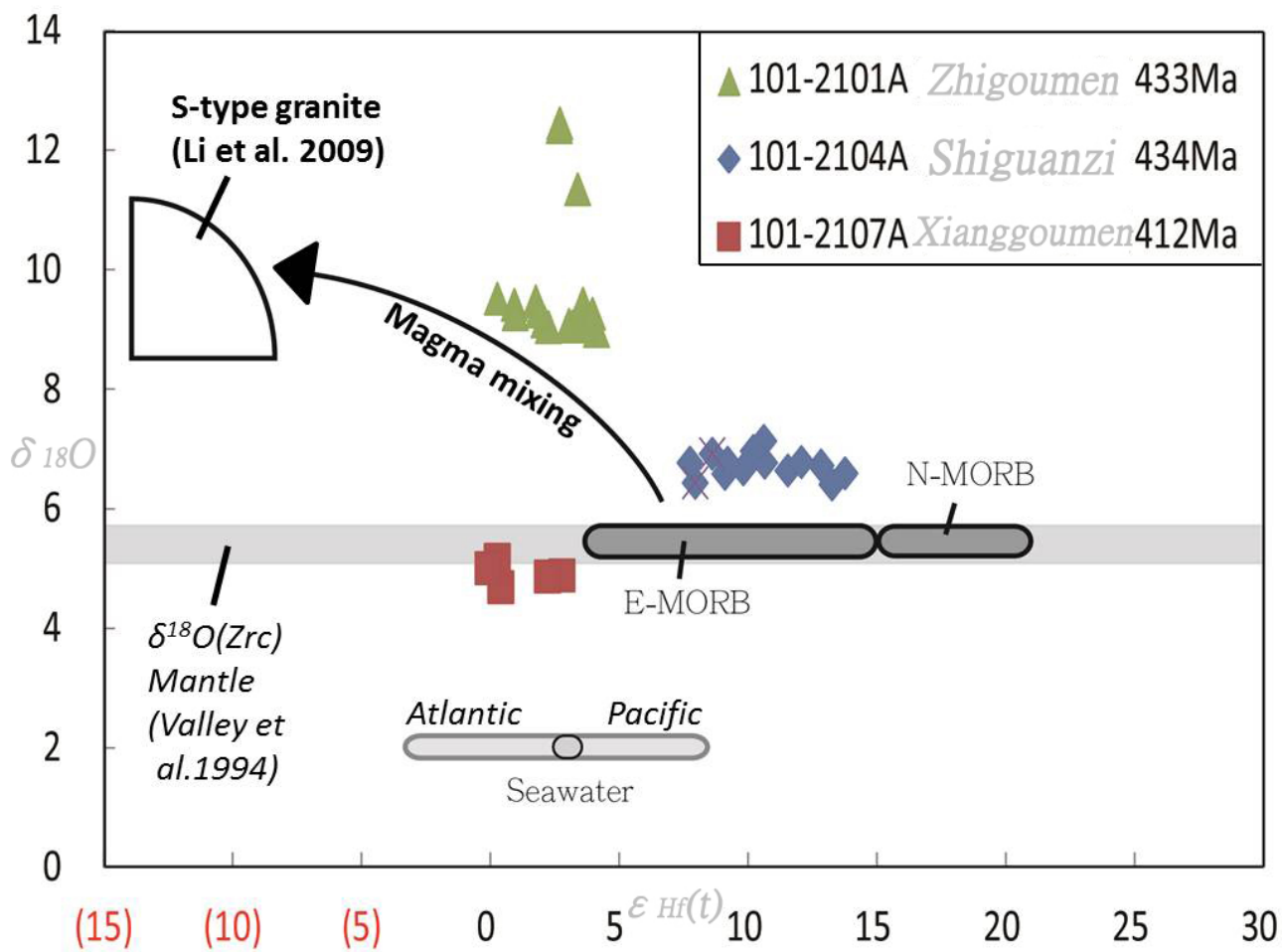
Field relationships, mineralogy, petrology, geochemistry, geochronology, and Nd-Hf-O isotopes of the ultramafic-mafic rocks from the east part of the Qilian block are studied in the present work. The Aganzheng intrusive body only exposed in the Zhigoumen, Shiguanzi, Xianggoumen outcrops and includes olivine pyroxenite, clinopyroxenite, pyroxene hornblendite, hornblendite, dioritic norite. The gabbroic and dioritic rocks are also layered or massive cumulates with rock types varying continuously from noritic gabbro through hornblende gabbro to dioritic norite. Contact metamorphic zones are well developed between the Aganzheng intrusive body and the country rock.

Major element contents of Aganzheng ultramafic-mafic rocks show subalkalic series and are characterized by low SiO<sub>2</sub> contents (38.09-54.96 %), low TiO<sub>2</sub> contents (0.09-0.72 %), low P<sub>2</sub>O<sub>5</sub> contents (0.00-0.36 %) and alkali contents (Na<sub>2</sub>O+K<sub>2</sub>O 0.01-5.35 %), but high MgO contents (9.68-33.06 %), Ni contents (116-1505 ppm), Cr contents (713-2808 ppm). Similar LREE-rich pattern ((Ce/Yb)<sub>N</sub> = 0.95-3.80 except two Samples) and tiny Eu anomaly (Eu/Eu\* = 0.6-1.2) indicate the Aganzheng ultramafic-mafic rocks have the same magma source. Trace elements are enriched in LILE (Rb, Th, U, K), relatively depleted in HFSE (Nb and Ta), and the La/Yb, Ce/Yb, Th/Yb, Nb/La, La/Sm values suggest the limited crustal contamination during the rise of the magma.

The  $\epsilon_{Nd}(430 \text{ Ma})$  values are  $-6.9$  to  $+2.5$  and  $T_{DM}$  values are 3.6–1.4 Ga. The SHRIMP ages are  $433 \pm 2$  Ma for the Zhigoumen pyroxenite (101-2101A),  $434 \pm 3$  Ma for Shiguanzi gabbro (101-2104A) and  $412 \pm 3$  Ma for the Xianggoumen serpentinite (101-2107A). In situ zircon O-Hf isotope, the  $\delta^{18}O$  compositions of vary from  $+9.03$  to  $+9.50$  (except three points  $+11.33$ ,  $+12.38$ ,  $+12.44$ ) and  $\epsilon_{Hf}(t)$  value is  $+0.29$  to  $+4.13$  for the Zhigoumen pyroxenite (101-2101A), the  $\delta^{18}O$  compositions of vary from  $+6.39$  to  $+7.12$  and  $\epsilon_{Hf}(t)$  value is  $+7.76$  to  $+13.26$  for Shiguanzi gabbro (101-2104A). and the  $\delta^{18}O$  compositions of vary from  $+4.68$  to  $+5.31$  and  $\epsilon_{Hf}(t)$  value of  $+0.28$  to  $+2.79$  for the Xianggoumen serpentinite (101-2107A).

According to the above datum, we suggest that middle Paleozoic magmatism last ~20 m.y. (434-412 Ma) on the northern margin of the Qilian Block was related to the Early Paleozoic continental collision between the Qilian and Qaidam blocks, and to subsequent subduction or thermal underplating.

Keywords: Ultramafic-mafic rock, SHRIMP, Nd-Hf-O isotope, Qilian Block, Underplating



## Zircon Hf isotopic constraints on the Jurassic-Oligocene magmatic rocks in the Lut-Sistan region, eastern Iran: Implications for the magmatic evolution

\*Han-Yi Chiu<sup>1,2</sup>, Sun-Lin Chung<sup>1,2</sup>, Mohammad Hossein Zarrinkoub<sup>3</sup>, Hao-Yang Lee<sup>1</sup>, Kwan-Nang Pang<sup>1</sup>, Seyyed Saeid Mohammadi<sup>3</sup>, Mohammad Mahdi Khatib<sup>3</sup>, Kuo-Lung Wang<sup>1</sup>

1. Institute of Earth Sciences, Academia Sinica, Taipei, Taiwan, 2. Department of Geosciences, National Taiwan University, Taipei, Taiwan, 3. Department of Geology, University of Birjand, Birjand, Iran

This study presents new zircon Hf isotopic results for 28 magmatic rocks of Jurassic-Oligocene ages in the Lut-Sistan region to better understand the magmatic evolution of eastern Iran before and after the Lut-Afghan collision. The Middle Jurassic (~168 Ma) granitoids yielded a wide range of zircon  $\varepsilon_{\text{Hf}}(\text{T})$  values from +8 to -1, revealing the similarity of variable isotopic feature of the coeval magmatic rocks forming along the Sanandaj-Sirjan zone, in agreement with the hypothesis of anti-clockwise rotation of the Lut block. The Early Cretaceous (113-107 Ma) gabbros that belong to the Birjand ophiolite indisputably show depleted mantle-derived zircon Hf isotope compositions of  $\varepsilon_{\text{Hf}}(\text{T})$  values from +16 to +12 and thus confirm their oceanic crustal origin. Another ~110 Ma diorite without ophiolitic affinity has relatively lower zircon  $\varepsilon_{\text{Hf}}(\text{T})$  values from +9 to +6, and it also contains abundant inherited zircons that show  $\varepsilon_{\text{Hf}}(\text{T})$  values between +5 and -2 at ~168 Ma, indicative of the widespread distribution of the Middle Jurassic magmatism in northern part of this region. In the Late Cretaceous, the emplacement of ~86 Ma granitoids also yielded depleted mantle-like zircon Hf isotopes of highly positive zircon  $\varepsilon_{\text{Hf}}(\text{T})$  values from +17 to +10, and the other granites yielded lower zircon  $\varepsilon_{\text{Hf}}(\text{T})$  values from +12 to +4 at 74-71 Ma. After the closure of the Sistan ocean during the Late Cretaceous (to Paleocene), the 57-53 Ma granitoids gave zircon  $\varepsilon_{\text{Hf}}(\text{T})$  values from +12 to +3 in the Early Eocene. Then, the zircon Hf isotopic results of extensive Eocene-Oligocene (46-24 Ma) magmatic rocks show a much variable signature of zircon  $\varepsilon_{\text{Hf}}(\text{T})$  values between +14 and -2, indicating the heterogeneity of widespread post-collisional magmas during this period. On the whole, the highly radiogenic zircon Hf isotopic features were mostly obtained from dated magmatic rocks in the Lut-Sistan region, similar to our recent observation on the magmatic rocks developed by the Neotethyan evolution in the Urumieh-Dokhtar magmatic arc, which suggest that the depleted-mantle component has played a critical role on the magmatic evolution since at least the Jurassic time.

Keywords: Zircon Hf isotopes, Lut-Sistan region, Iran, magmatic evolution

# Petrological and Geochemical Study of Sundoro Volcano, Central Java, Indonesia: Temporal Variations in Differentiation and Source Processes in the Growth of an Individual Arc Volcano

\*Haryo Edi Wibowo<sup>1,2</sup>, Mitsuhiro Nakagawa<sup>1</sup>, Ryuta FURUKAWA<sup>3</sup>, Akira Takada<sup>3</sup>, Oktory Prambada<sup>4</sup>

1. Department of Natural History of Science, Faculty of Science, Hokkaido University, Japan, 2. Geological Engineering Department, Faculty of Engineering, Gadjah Mada University, Indonesia, 3. Geological Survey of Japan, National Institute of Advanced Industrial Science and Technology, Japan, 4. Center of Volcanological and Geological Hazard Mitigation, Ministry of Energy and Mineral Resources, Indonesia

We reported new Sr-Nd-Pb radiogenic isotope ratios in addition to the complementing whole rock geochemistry and trace elements combined with mineral chemistry of representative rocks of Sundoro volcano, central part of Java sector of Sunda arc. Collected samples represent stratigraphically well-constrained volcanic products from 34 to 1 ka activities. The rocks of the volcano span from basalt (SiO<sub>2</sub> 51.5 wt. %) to andesite (62.9 wt.%) and are dominated by basaltic andesite. Least evolved rocks contain MgO less than 6 wt.% and are considered as evolved basalt. The rocks can be grouped into three magma types on the basis of isotopic compositions. The three magma types are named A-, B-, and C-type and characterized by low, medium, and high Sr-Pb isotopic compositions, respectively, which are in tune with variations of Ba/Zr, La/Yb, and Th/Yb ratios.

Against progressive silica content, evolution trend of the three magma types are separated: relatively parallel to each other in <sup>87</sup>Sr/<sup>86</sup>Sr, ratios of Ba/Zr, and La/Yb, diverge in ratios of Th/Yb, and discretely varied in Pb-isotope. Combination of these discrete geochemical evolution trends with petrographic disequilibrium features and wide-range bimodal compositions of plagioclase crystal core (An<sub>46-94</sub>) suggest that 1) magma mixing is dominant process in intra-crustal level. 2) The three magma types correspond to mixing of three distinct couples of mafic- and felsic-end member magmas. 3) The felsic end-member magma cannot be produced from fractionation of corresponding mafic end-member magma and might come from different melt source. 4) The three mafic-end member magmas are not related co-genetically, thus relative correlation of their mafic rocks might represent magma source characteristics. Trace elements as proxies of slab contributions (e.g. Ba/Zr, Th/Yb, La/Yb) of the representative mafic rocks of the three magma types show positive correlation to Sr- and Pb-isotopic compositions but negative to Nd-isotopic ratios. We proposed that magma of A-, B-, and C-type corresponds to three distinct slab-derived fluxes containing sediment-derived melt contributions approximately 50%, 55%, and 60%, respectively, which were added to the mantle wedge in a rates of ~1%, ~1.5%, and ~2%, respectively. Temporal variations of the magma type shows the existence of A-type in 20-9 ka, co-existence of A- and B-type in 14-17 ka, and abrupt change from A- to C-type after 9 ka. Reconstruction of the supply magma system in these periods indicate that time interval between the three slab-derived fluxes is about 3-8 ky and shows increasing portion of sediment contribution and rate of slab-fluxes through time. Further application of these approaches to dataset of Merapi volcano revealed increasing rate of slab-derived flux to the magma genesis beneath volcanic front region of central part of Java through time.

Keywords: Sunda arc, Temporal variation, Multiple magmas, Slab contribution, Sundoro volcano